WCAP-14092

PHASE IVb WIND TUNNEL TESTING FOR THE WESTINGHOUSE AP600 REACTOR

G. R. Lythe
D. Surry

BLWT-SS6-1994

BOUNDARY LAYER WIND TUNNEL LABORATORY
THE UNIVERSITY OF WESTERN ONTARIO
FACULTY OF ENGINEERING SCIENCE
LONDON, ONTARIO, CANADA
N6A 5B9

TABLE OF CONTENTS

SUMMARY

This report details the second part of the fourth phase of the wind tunnel testing of the Westinghouse AP600 nuclear reactor (there was no Phase III). The design for this reactor employs passive means for emergency cooling, including natural draft cooling and water film evaporative cooling. This cooling is dependent on natural convection through the building, which could be affected by wind conditions. Phase I testing examined the wind effects of various changes in the geometry of the containment building and its surroundings. Phase I testing is detailed in Reference 8. Phase II testing included the modelling of the complete flow path within the building and was used primarily to provide information for the design of the baffle wall. This testing is detailed in Reference 9. Phase IVa testing included testing a large model in another, faster wind tunnel in order to examine Reynold's number effects. As well, measurements were taken to provide final baffle wall design loads (subject to the results of this study), to examine the effects of the hyperbolic cooling tower, to examine the effects of a uniform velocity profile and to provide some information for the modelling of the cooling tower in this phase. Phase IVa testing is detailed in Reference 10.

The aims of this phase of the testing are to examine the effects of severe terrain on the baffle loads. The configurations tested include:

1. The base case, consisting of the complete AP600 plant, including a single hyperbolic cooling tower;

2. The base case with two cooling towers;

3. With a nearby escarpment;

4. With a nearby escarpment and a mountain backdrop;

5. In a river valley; and,

6. In a river valley, with two cooling towers.

In order to allow the modelling of large areas of terrain, a smaller scale of 1:800 was chosen. It is expected that the magnitudes of the results may not be as accurate as previous tests, but the comparison between cases will be valid. This may result in factors that could be applied to the baffle loads determined in Phase IVa. Initial testing was performed to ensure that the wake characteristics of the cooling tower were appropriately modelled, based on measurements taken at a larger scale in Phase IVa. The test model was instrumented for pressure measurements at 44 locations (plus 16 on the cooling tower) and was tested in turbulent boundary layer flow conditions. The approach flow was representative of a flow in an open country terrain (i.e., ANSI exposure C), and was further modified by the terrain models surrounding the site.

The highlights and main findings of the study are as follows:

1. In most of the configurations, the largest peak inlet-minus-chimney pressure changes very little from the base case. In the river valley case with two cooling tower, however, this pressure increases by a factor of 1.14, for a small range of wind angles. Thus, the base case baffle loads are bounding except for the river valley case with two cooling towers.

2. The effect of mountains and/or an extra cooling tower is to reduce the inlet-minus-chimney pressure for wind directions with the mountains and/or cooling towers upstream of the plant. In all cases, the mean inlet-minus-chimney pressure remains positive. The duration of negative inlet-minus chimney pressure fluctuations becomes longer for the wind directions with mountains and/or

design wind speed was 12 seconds, versus 2 seconds for the base case. For the wind angle with the most negative fluctuations in the river valley case, the inlet-minus-chimney pressure was in the negative 68% of the time, versus 4.5% of the time for the base case.

1· INTRODUCTION

The Westinghouse AP600 nuclear reactor is designed to use passive means for emergency cooling. These include natural draft and water film evaporative cooling which are made possible by an air flow path through the containment building. The air flows in inlets at the top of the building, downwards past a baffle wall, then around the bottom of the baffle, upwards between the baffle and the containment vessel and out the chimney at the top of the building.

A goal of the design is that the wind not resist the air flow through the building. Phase I testing, detailed in reference 7, examined the effects of various design changes on the wind-induced pressures. In that testing , the flow through the building was not modelled, but the pressure difference between inlets and chimney (i.e. the pressure driving any flow) was measured. In the Phase II tests, reported in reference 9, the air flow path was modelled for two different building designs: the most wind neutral design found in Phase I testing, and the current design of the building. The purpose of the Phase II testing was primarily to provide information for the design of the baffle wall. The information sought was the loads on the wall and how uniform the flow was at various points along the flow path. Buoyancy was not considered since the driving pressure due to buoyancy amounts to only about 1 to 5% of the wind-induced driving pressure for the design wind cases.

At the end of Phase II, there remained several outstanding questions. First, the effect of Reynolds number on the results. This could only be addressed definitively by testing a larger model in a faster wind tunnel such that the Reynold's numbers were in the same range as expected full scale values. Secondly, the effect of a tornado wind profile (near uniform) on the results. This could be accomplished using the same test model as in previous phases, but with a different flow model. Thirdly, the effects of the hyperbolic cooling tower on the results. Some limited measurements were made in Phase II; however, the blockage of the cooling tower in the University of Western Ontario (UWO) wind tunnel was excessive. This question could be addressed by testing the 1:96.67 model in a larger wind tunnel where the blockage would be small. Phase IVa (there was no phase III), was aimed at addressing these questions.

The final outstanding question, the effect of severe terrain, is the subject of the current Phase IVb. For this phase, a smaller scale, 1:800, was chosen to allow the modelling of larger areas around the site. At this scale, however, the Reynold's numbers are much smaller than full scale values which could lead to results whose values are not representative of full scale. This is perfectly acceptable here, since it is the *difference* between cases that is of interest and these differences should still be valid. Nevertheless, it is important to properly model the wake characteristics of the hyperbolic cooling tower, even if this means distorting the shape or scale of the tower with respect to the rest of the site. With this in mind, measurements of the wake characteristics behind the cooling tower were taken during phase IVa, on a 1:96.67 scale model of the cooling tower in the 30' x 30' wind tunnel at the National Research Council of Canada (NRC). These measurements were then used as the basis for modelling the wake characteristics in the current phase.

2· EXPERIMENTAL PROCEDURE - COOLING TOWER MODELLING

2·1 Preliminary Measurements at the NRC Wind Tunnel

A 1:96.67 scale model of the cooling tower was built as part of Phase IVa. Photographs of the model in the wind tunnel are shown in Figure 1 (note that the other models shown were not present during the tests on the cooling tower). It was instrumented for pressure measurements at 16 locations around the throat of the tower. The

numbering system for these pressure taps is shown in figure 2. The model was mounted near the centreline of the wind tunnel and was tested in a 1:96.67 scale boundary layer representative of open country conditions (ANSI exposure C). A description of the flow modelling is given in section 4.1 of reference 10.

Two types of tests were performed: measurements of the pressures around the throat of the cooling tower, and measurements of speeds in the wake of the tower. All pressure data were measured using a solid state pressure scanner system which sampled pressures at a rate approximating 4.5 samples per second in full scale for a period approximating 26 minutes in full scale (the time scale used here is based on the full scale design wind speed of 214 mph at the top of the chimney - a slower wind speed would yield a longer record with fewer samples per second). All of these samples are kept for later analysis (e.g. to determine the maximum, minimum, mean and rms values in each case). During the tests, the speed, denoted Vref, was monitored by a pitot-static tube mounted just downstream of the test model, at a height well above the test model. All of the pressure data are presented in this report in the form of non-dimensional pressure coefficients as defined in reference 1. They are referenced to the mean dynamic pressure at the containment building roof height, $1/2\ \rho V^2$roof, where Vroof is calculated from the Vref measured during the test using a Vroof/Vref ratio measured in a separate experiment after the testing.

The second type of test was the measurement of speeds in the wake. In this test, a hot-wire sensor was mounted on a traversing mechanism at a distance downstream from the cooling tower equal to the distance to the centreline of the containment building. A horizontal traverse was made across the cooling tower wake at the height of the top of the containment building chimney. Both the mean speed and the longitudinal component of the turbulence intensity were measured.

2.2 Modelling of the Wind at the UWO Wind Tunnel

The basic tool for these tests was the Laboratory's Boundary Layer Wind Tunnel, which allows extended fetches of coarsely modelled upstream terrain to be placed in front of the building under test. The wind tunnel flow then develops boundary layer characteristics representative of those found in full scale. This methodology has been highly developed and is detailed elsewhere (1,2,3). In this case, a 1:800 scale boundary layer representative of open country conditions (ANSI exposure C) was required. This was achieved using floor roughness with a height of 0.5 inches. The upstream terrain model is shown in Figure 3.

Vertical profiles of mean speed and the longitudinal component of the turbulence intensity, measured immediately upstream of the proximity model, are shown in Figure 4 compared with reference profiles for open country terrain. The latter have been developed by ESDU (4,5,6) through fitting theoretical models to available full scale data. The roughness length, z_0, (a characteristic parameter of the mean speed profile) calculated from the wind tunnel data is approximately 0.02 metres. This is well within the acceptable range of a factor of 2 from the accepted median open country value of 0.03. The ratios of mean speeds at particular heights to those at roof height are shown in Table 1, along with similar reference values. Also shown are values of the local turbulence intensity, which is simply the root-mean-square (rms) speed divided by the mean speed at each height. The table includes heights up to 1.5 times the building height. The table shows that, except for the few points closest to the ground, the mean ratios are within 0.05 of the reference values and the local intensities are within 2 percentage points of the ESDU values. Hence this is a very good representation of the wind structure for an open country terrain.

The simulation was further checked by measuring a spectrum of the wind speed at roof height. This spectrum is shown in Figure 5, along with the reference spectrum for open country terrain. The figure shows that the spectrum is well within the acceptable range of a factor of 2 over the entire range of wave numbers.

2.3 Measurements at UWO

It was expected that some distortion in the modelling of the cooling tower may have been necessary in order to model its wake characteristics properly at the 1:800 scale. Some initial tests on several crudely

constructed models indicated that the best modeling of the wake characteristics was achieved without any distortion of the model -i.e. simply scaling the model at 1:800. With this knowledge, a more precise model of the cooling tower was constructed and instrumented for pressure measurement at the same 16 locations that were used for the NRC tests (see figure 2).

As with the tests at NRC, two types of tests were performed; measurements of the pressures around the throat of the cooling tower, and measurements of speeds in the wake of the tower. All pressure data were measured using a solid state pressure scanner system which sampled pressures at a rate approximating 3 samples per second in full scale for a period approximating 63 minutes in full scale (the time scale used here is based on the full scale design wind speed of 214 mph (Appendix D of Reference 9) at the top of the chimney - a slower wind speed would yield a longer record with fewer samples per second). All of these samples are kept for later analysis (e.g. to determine the maximum, minimum, mean and rms values in each case). During the tests, the speed, denoted Vref. was monitored by a pitot-static tube mounted just upstream of the proximity model, at a height near the roof of the wind tunnel. All of the pressure data are presented in this report in the form of non-dimensional pressure coefficients as defined in reference 1. They are referenced to the mean dynamic pressure at roof height, $1/2\ \rho V^2$ roof, where Vroof is calculated from the Vref measured during the test using the Vroof/Vref ratio from the measured velocity profile.

The second type of test was the measurement of speeds in the wake. In this test, a hot-wire sensor was mounted on a traversing mechanism at a distance downstream from the cooling tower equal to the distance to the centerline of the containment building. A horizontal traverse was made across the cooling tower wake at the height of the containment building chimney. both the speed and the longitudinal component of the turbulence intensity were measured.

3 EXPERIMENTAL RESULTS AND DISCUSSION - COOLING TOWER MODELLING

Figure 6 shows a comparison of the mean pressure distributions around the throat of the cooling tower measured in both wind tunnels. The coefficients shown have been normalized in both cases by appropriate dynamic pressures that give a coefficient of 1.0 at the stagnation point. The two sets of data compare very well, indicating that the drag characteristics, and hence the wake characteristics, of the two models are similar. An approximate drag coefficient per unit height can be calculated from these data; for the NRC data it is 0.42 and for the UWO data it is 0.39. The agreement here is also very good.

The results of the speed measurements behind the cooling tower are shown in figure 7; figure 7a shows mean speeds; figure 7b shows turbulence intensities, and figure 7c shows peak speeds formed from the measured mean and rms speeds. All speeds are normalized by the largest mean speed measured in the traverse. The speed measurements indicate that the width of the wakes and the turbulence intensities are similar in both cases, but the reduction in mean speed behind the cooling tower is not quite as large in the UWO tests as in the NRC tests. As a result, the peak speeds are somewhat higher behind the tower in the UWO tests, which will lead to somewhat conservative results. It is interesting to note that the results presented here, while conservative, are not as good as the initial preliminary results measured behind the coarsely modelled cooling towers.

4 EXPERIMENTAL PROCEDURE - MAIN TESTS

4.1 Modelling of the Containment Building and the Surroundings

The basic tool for these tests was the Laboratory's Boundary Layer Wind Tunnel. The 1:800 scale model of the AP600 plant was placed at the center of the turntable and was surrounded by a "proximity" model consisting of the particular terrain mode. for the configuration being tested. This entire assemblage could be rotated to simulate different wind directions. The model scale of 1:800 was chosen to allow a relatively large area of terrain to be included in the proximity model. Close-up views of the test model are shown in figure 8.

Tests were performed for the following configurations:

1. The base case, consisting of the complete AP600 plant, including a single hyperbolic cooling tower;

2. The base case with two cooling towers;

3. With a nearby escarpment. The escarpment is 100' high with a 1:10 slope. The top of the escarpment is 500' from the center of the cooling tower.

4. With a nearby escarpment and a mountain backdrop. The mountain begins 1200' east from the center of the shield building and rises to a height of 1000';

5. In a river valley. This consists of the mountain backdrop as in 4, with another 1000' mountain 2800' to the west of the center of the shield building. The escarpment is filled in; and,

6. In a river valley, with two cooling towers.

A sketch showing the important dimensions is presented in Figure 9a. Photographs showing configurations 3 to 6 are shown in figure 9b. For configurations 1 and 2, a simple proximity model consisting of flat sheets of plywood were used.

4.2 Pressure Measurements

All pressure data were measured using a solid state pressure scanner system which sampled pressures at a rate approximating 3 samples per second in full scale for a period approximating 63 minutes in full scale (the time scale used here is based on the full scale design wind speed of 214 mph at the top of the chimney - a slower wind speed would yield a longer record with fewer samples per second). All of these samples are kept for later analysis (e.g. to determine the maximum, minimum, mean and rms values in each case). During the tests, the speed, denoted Vref, was monitored by a pitot-static tube mounted just upstream of the proximity model, at a height near the roof of the wind tunnel. All of the pressure data are presented in this report in the form of non-dimensional pressure coefficients as defined in reference 1. They are referenced to the mean dynamic pressure at roof height, $1/2\ \rho V^2$ roof, where Vroof is calculated from the Vref measured during the test using the Vroof/Vref ratio from the measured velocity profile which was measured just upstream of the proximity model with no proximity model in place.

Pressures were measured at the locations shown in Figure 10. As well, several combinations of the pressure measurements were made at each sampling instant to form data records for new "combination" taps:

1. Tap 701 represents the average of the inlet taps;

2. Tap 702 represents the average of the chimney taps;

3. Tap 703 represents the difference between the average of the inlet taps and the average of the chimney taps.

As well, readings were taken from the taps on the cooling tower, but were not subsequently used.

5. EXPERIMENTAL RESULTS AND DISCUSSION

5.1 General

For all tests, statistics of the pressure coefficient records (maximum, minimum, mean and rms) have been determined for all taps and are tabulated in Appendix A. Taps are numbered in accordance with the numbering system shown in Figures 2 and 10. These data are examined more closely in the following sections.

The choice of 1:800 scaling, as dictated by the large area models, means that the Reynolds numbers for the shield building and chimney were substantially reduced below those for previous tests. This choice was made on the basis that the primary results were to be comparative rather than absolute; however, previous tests also indicated a lack of Reynolds number sensitivity, presumably due to the flow separations from the top of the chimney and from the "shoulders" of the shield building being more important than the sides of the shield building. To examine whether this insensitivity extended to this 1:800 model, comparisons with previous data have been made. Figure 11 shows comparisons with Phase IVa data: Figure 11a shows comparisons for taps in the inlets and chimney, and Figure 11b shows comparisons for the "combination" taps. The agreement is remarkable good, considering the large difference in Reynold's numbers between the tests. This indicates that the results of interest are relatively insensitive to Reynold's numbers over this range. Another observation that can be made from these comparisons is the effect of the cooling tower, since it is present in the current data, but was not for the Phase IVa inlet-minus-chimney pressures, which in turn would indicate lower baffle loads. Figure 12 shows a plot of the first 5 minutes (full scale) of the data record for the three "combination" taps for the wind angle 280° where the effect of the cooling tower appears to be the strongest. Over the entire data record (63 minutes), the inlet-minus-chimney pressure was negative 4.5% of the time. Figure 13 shows a histogram of the number of times over the entire data record that the duration of the negative inlet-minus-chimney pressure was equal to various values. The figure shows that most of the time, the pressure is negative for only a very short time. The longest time that the pressure stayed negative was less than 2 seconds. Note that the time scale used for Figures 12 and 13 is based on a full scale design wind speed of 214 mph at the top of the chimney - slower wind speeds would yield longer durations.

In the following section, data from the various configurations are compared with each other. Data from the three "combination" taps are shown (see above for the definition of the "combination" taps).

5.2 Main Results

Figure 14 shows the effect of adding a second cooling tower to the base case, which already includes one cooling tower. The effect is very similar to the effect of the first cooling tower, but shifted to the wind angles where the second cooling tower is upstream - that is, mean pressures are reduced and rms pressures remain similar. The net result is to reduce baffle loads. The effect on negative inlet-minus-chimney pressure is similar to that discussed above for a single cooling tower.

Figure 15 shows the effect of a nearby escarpment. In this figure, differences over azimuths from 0° to 180° can be attributed to speed-ups over the built-up portion of the surrounding terrain model and hence are not valid for design. For azimuths 190° to 350°, however, the differences are due only to the escarpment. The escarpment tends to increase both the inlet and the chimney pressures over this azimuth range; however, when the difference between inlet and chimney pressure is looked at, the effect of the escarpment largely cancels out. The ratio of the largest peak inlet-minus-chimney pressure over this azimuth range from the escarpment case to

that from the base case is 1.01, indicating that the baffle loads would be similar in both cases (these do not occur for the same wind angle).

Figure 16 shows the effect of a nearby escarpment with a mountain backdrop. Again in this case, the largest peak inlet-minus-chimney pressure is almost unchanged from the base case, although it occurs at a different wind angle. In this case however, the mountain causes larger peak negative inlet-minus-chimney pressures. Figure 17 shows a plot of the first 5 minutes (full scale) of the data record for the three "combination" taps for the wind angle 90° where the effect of the mountain appears to be the strongest. Over the entire data record (63 minutes), the inlet-minus-chimney pressure is negative 31% of the time. Figure 18 shows a histogram of the number of times over the entire data record that the duration of the negative inlet-minus-chimney pressure was equal to various values. The figure shows that most of the time, pressure is negative for only a short time. The longest time that the pressure stayed negative was less than 14 seconds. Note that the time scale used Figures 17 and 18 is based on a full scale design wind speed of 214 mph at the top of the chimney - slower wind speeds would yield longer durations.

Figure 19 shows the effect of a river valley site. In this case, the largest peak inlet-minus chimney pressure is reduced slightly form the base case, by a factor of 0.92. In this case, as in the previous case, the mountains cause larger peak negative inlet-minus-chimney pressures. Figure 20 shows a plot of the first 5 minutes (full scale) of the data record for the three "combination" taps for the wind angle 70° where the effect of the mountains appears to be the strongest. Over the entire data record (63 minutes), the inlet-minus-chimney pressure is negative 68% of the time. Figure 21 shows a histogram of the number of times over the entire data record that the duration of the negative inlet-minus-chimney pressure was equal to various values. The figure shows that most of the time, the pressure is negative for only a short time. The longest time that the pressure stayed negative was less than 12 seconds. Note that the time scale used for Figures 20 and 21 is based on a full scale design wind speed of 214 mph at the top of the chimney - slower wind speeds would yield longer durations.

Figure 22 shows the effect of adding a second cooling tower to the river valley site configuration. The second cooling tower has little effect, although the largest peak inlet-minus-chimney pressure is now slightly larger than the base case, by a factor of 1.14. This only occurs over a wind section of 20°. it should be noted that the mountain cases examined here, including this case, are particularly severe since the mountains are of limited length, causing severe conditions for glancing wind angles.

REFERENCES

1. Davenport, A.G. and Isyumov, N., "The Application of the Boundary Layer Wind Tunnel to the Prediction of Wind Loading", International Research Seminar on Wind Effects on Buildings and Structures, Ottawa, Canada, September 1967, University of Toronto Press, 1968.

2. Whitbread, R.E., "Model Simulation of Wind Effects on Structures", NPL International Conference on Wind Effects on Buildings and Structures, Teddington, England, 1963.

3. Surry, D. and Isyumov, N., "Model Studies of Wind Effects - A Perspective on the Problems of Experimental Technique and Instrumentation", ICIASF-75, Ottawa, Sept. 1975.

4. ESDU, "Characteristics of atmospheric turbulence near the ground. Part I: definitions and general information", Item number 74030, ESDU International Ltd., London, England, 1974.

5. ESDU, "Characteristics of atmospheric turbulence near the ground. Part II: single point data for strong winds (neutral atmosphere)", Item no. 85020, ESDU International Ltd., London, 1985.

6. ESDU, "Strong winds in the atmospheric boundary layer. Part I: mean hourly wind speeds", Item no. 83026, ESDU International Ltd., London, England, 1982.

7. Stewart, W.A. and Pieczynski, A.T., "Tests of Air Flow Path for Cooling the AP600 Reactor Containment", Westinghouse Electric Corporation, Report 88-8E9-ADLWR-R2, March 28, 1988.

8. Lythe, G.R. and Surry, D., "Phase I Wind Tunnel Testing for the Westinghouse AP600 Reactor", The University of Western Ontario, BLWT-SS36-1991 (WCAP-13294, Westinghouse Proprietary Class 2)

9. Lyth, G.R. and Surry D., "Phase II Wind Tunnel Testing for the Westinghouse AP600 Reactor", The University of Western Ontario, BLWT-SS15-1992 (WCAP-13323, Westinghouse Proprietary Class 2)

10. Lythe, G.R. and Surry, D., "Phase IVa Wind Tunnel Testing for the Westinghouse AP600 Reactor", The University of Western Ontario, BLWT-SS4-1994 (WCAP-14068, Westinghouse Proprietary Class 2)

The information contained in the following Table, Figures, and Appendix is classified Westinghouse Proprietary Class 2, and thus, has been excluded from this non-proprietary version of this report:

TABLE:

1 Comparison of Velocity and Turbulence Intensity Profiles for the UWO Tests

FIGURE:

4 Vertical Profiles of Mean Wind Speed and Turbulence Intensity Compared with Theoretical Profiles for Open Country Terrain - UWO 1:800 Tests
5 Spectrum of Velocity at Roof Height Compared with Theoretical Spectrum for Open Country Terrain - UWO 1:800 Tests
6 Distribution of Mean Pressure Coefficients Around the Throat of the Cooling Tower
7a Horizontal Profile of Mean Velocity Behind the Cooling Tower at the Containment Building Roof
7b Horizontal Profile of Intensity Behind the Cooling Tower at the Containment Building Roof
7c Horizontal Profile of Peak Velocity Behind the Cooling Tower at the Containment Building Roof
9a Sketch Showing the Important Dimensions of the Model
11a Comparison of Pressure Coefficients Between Phase IVa and IVb Testing
11b Comparison of Pressure Coefficients Between Phase IVa and IVb Testing
12 Time History of Pressure Coefficients; Base Case, Azimuth 280°
13 Histogram of Durations of Negative Inlet-Minus-Chimney Pressures; Base Case, Azimuth 280°
14 Comparison of Pressure Coefficients; Base Case vs. Base Case with Two Cooling Towers
15 Comparison of Pressure Coefficients; Base Case vs. Escarpment Case
16 Comparison of Pressure Coefficients; Base Case vs. Escarpment with Mountain Backdrop
17 Time History of Pressure Coefficients; Escarpment with Mountain Backdrop, Azimuth 90°
18 Histogram of Durations of Negative Inlet-Minus-Chimney Pressures; Escarpment with Mountain Backdrop, Azimuth 90°
19 Comparison of Pressure Coefficients; Base Case vs. River Valley Case
20 Time History of Pressure Coefficients; River Valley Case, Azimuth 70°
21 Histogram of Durations of Negative Inlet-Minus-Chimney Pressures; River Valley Case, Azimuth 70°
22 Comparison of Pressure Coefficients; River Valley Case vs. River Valley Case with Two Cooling Towers

APPENDIX:

A Calibration of Flow Losses

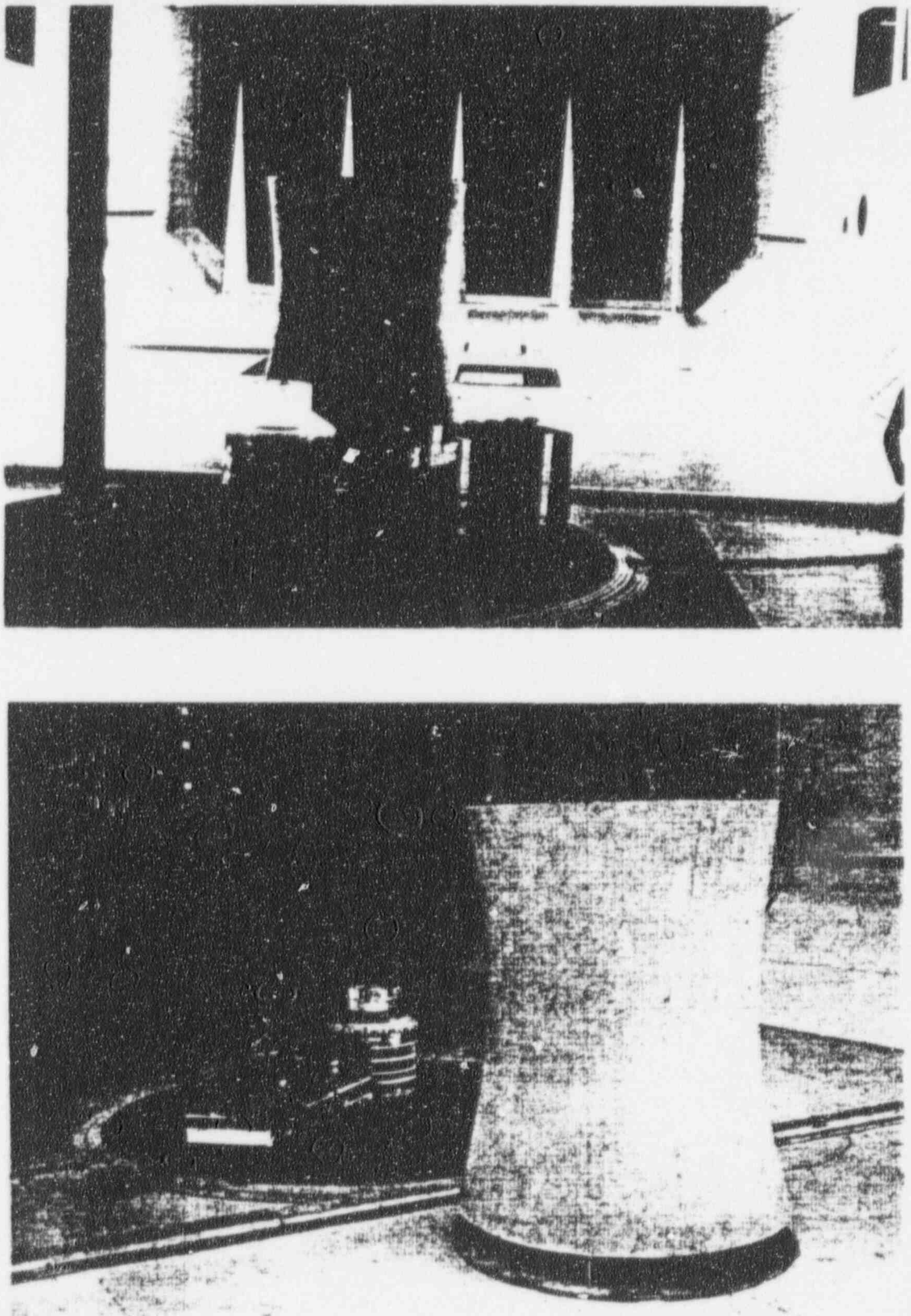

FIGURE 1 PHOTOGRAPHS OF THE COOLING TOWER MODEL IN THE WIND TUNNEL
NRC 1:96.67 TESTS

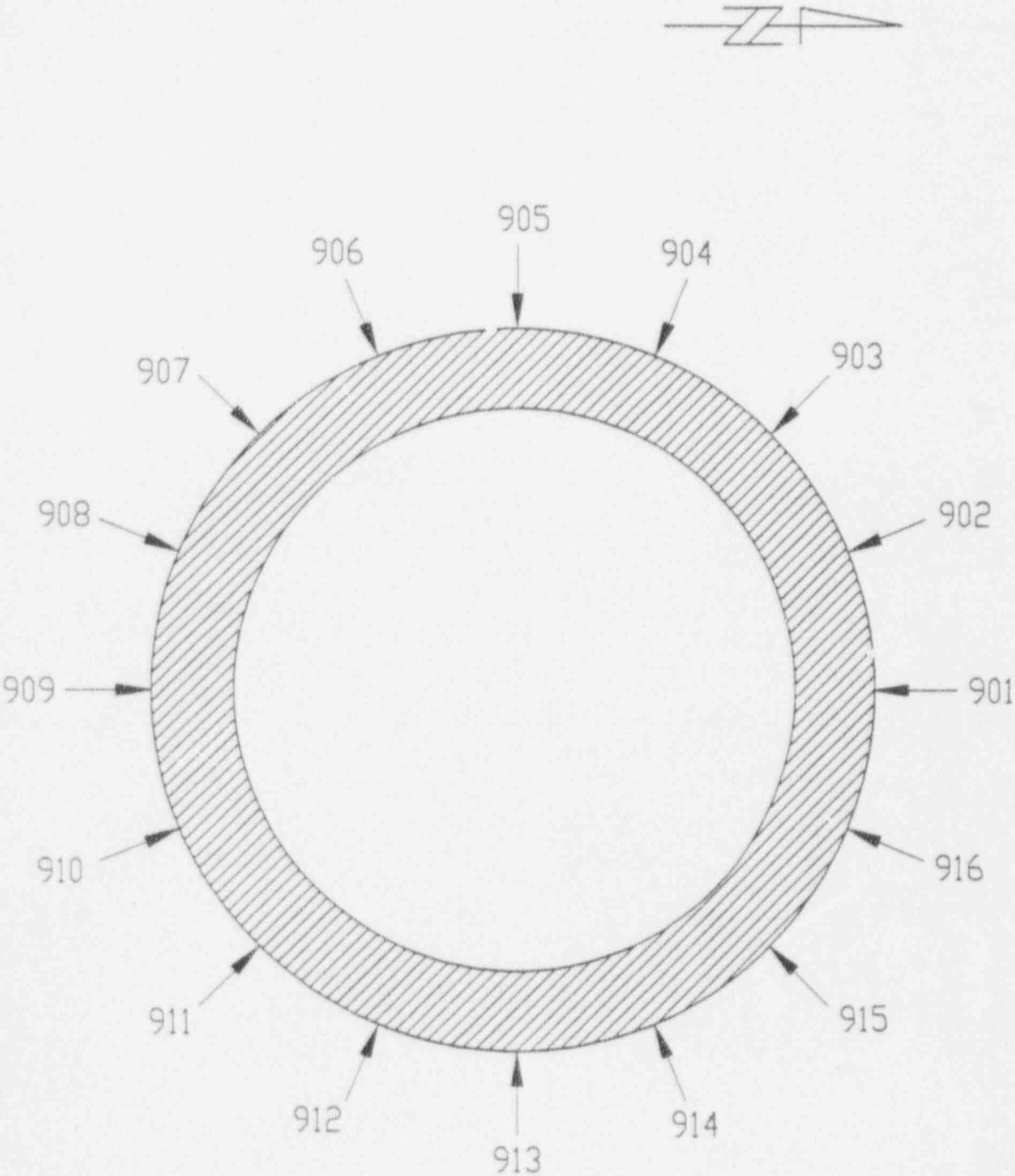

FIGURE 2 HORIZONTAL SECTION THROUGH THE COOLING TOWER MODEL AT THROAT HEIGHT SHOWING PRESSURE TAP NUMBERING

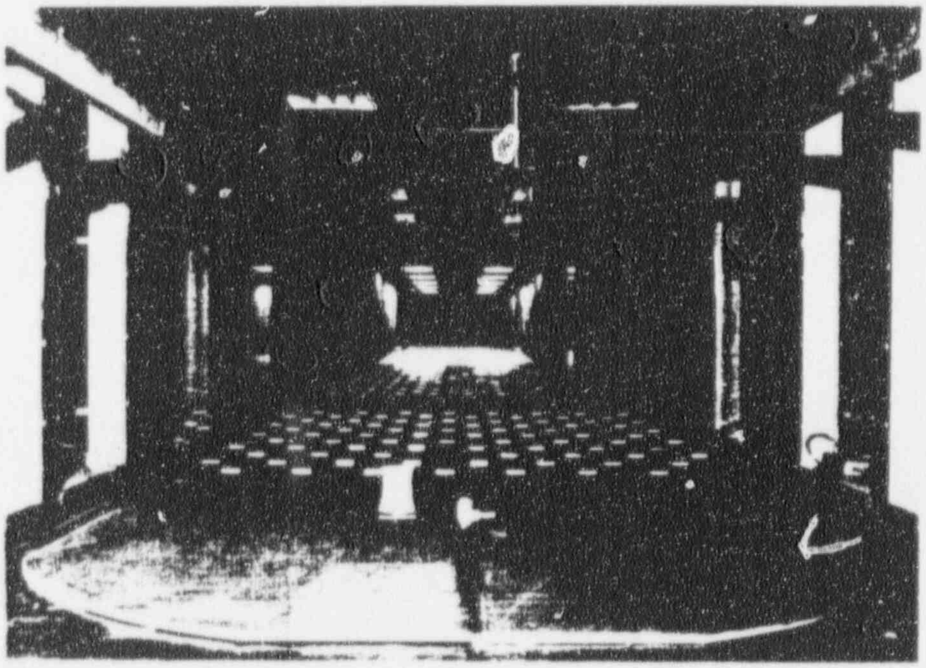

FIGURE 3 VIEW OF THE MODEL IN THE WIND TUNNEL SHOWING THE UPSTREAM TERRAIN MODEL USED
UWO 1:800 TESTS

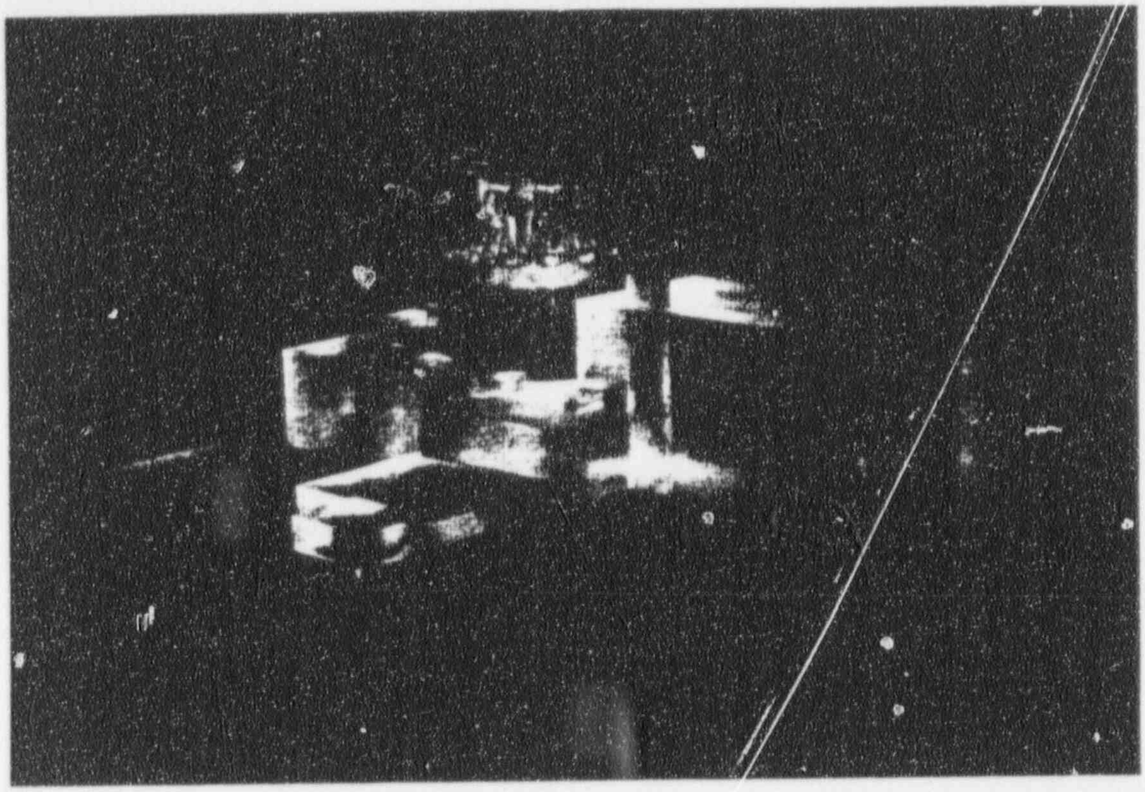

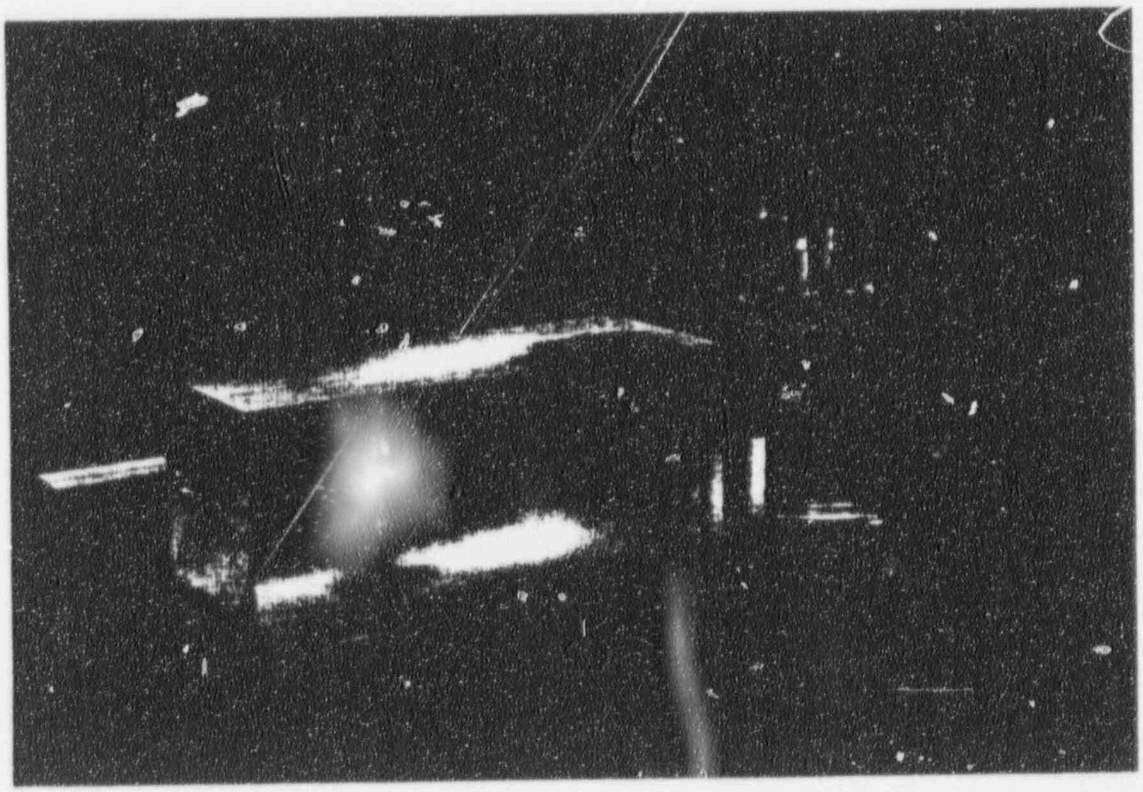

FIGURE 8a CLOSE-UP VIEWS OF THE 1:800 TEST MODEL

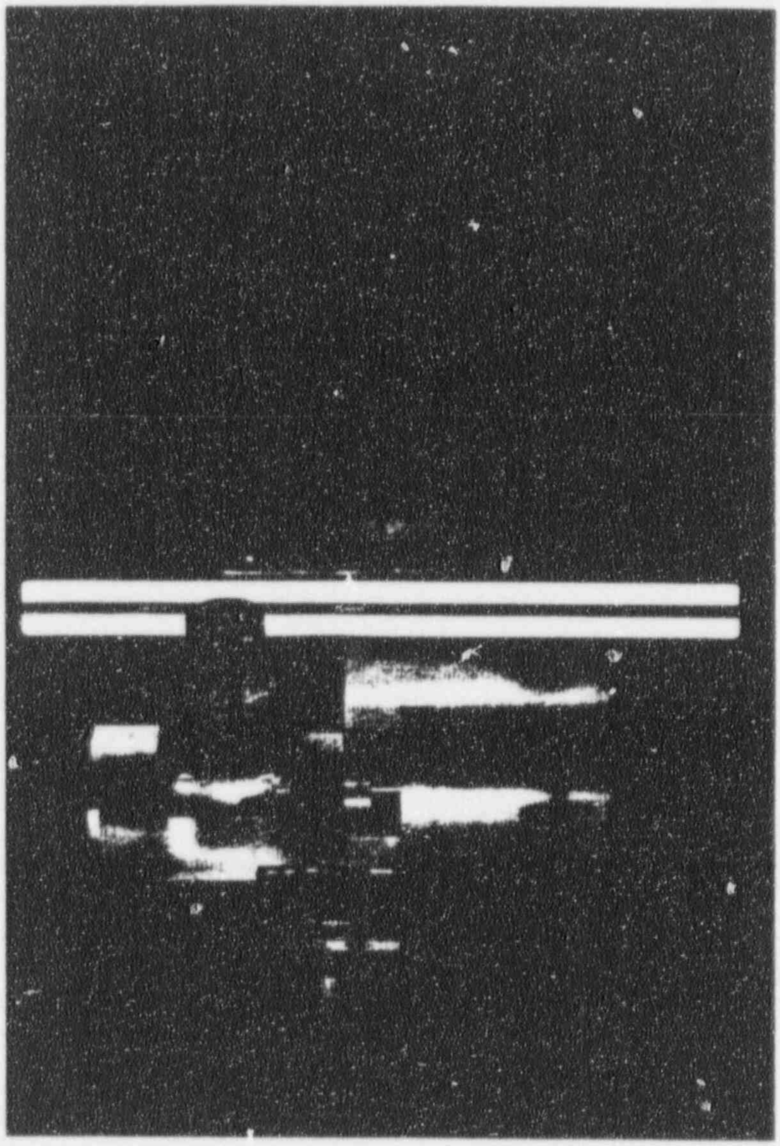

FIGURE 8b   CLOSE-UP VIEW OF THE 1:800 TEST MODEL

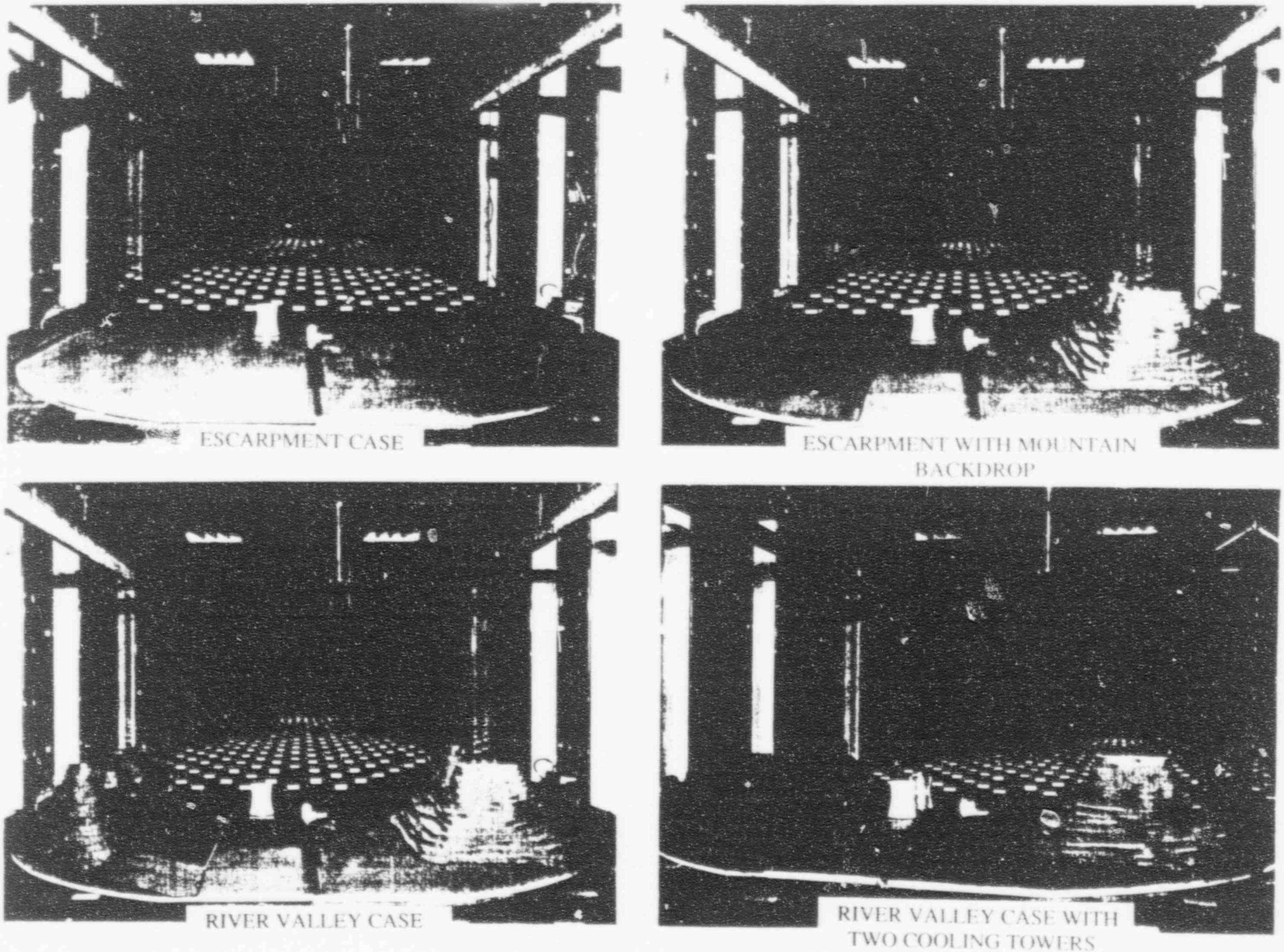

FIGURE 9b VIEWS OF THE MODEL IN THE WIND TUNNEL SHOWING SEVERAL OF CONFIGURATIONS TESTED

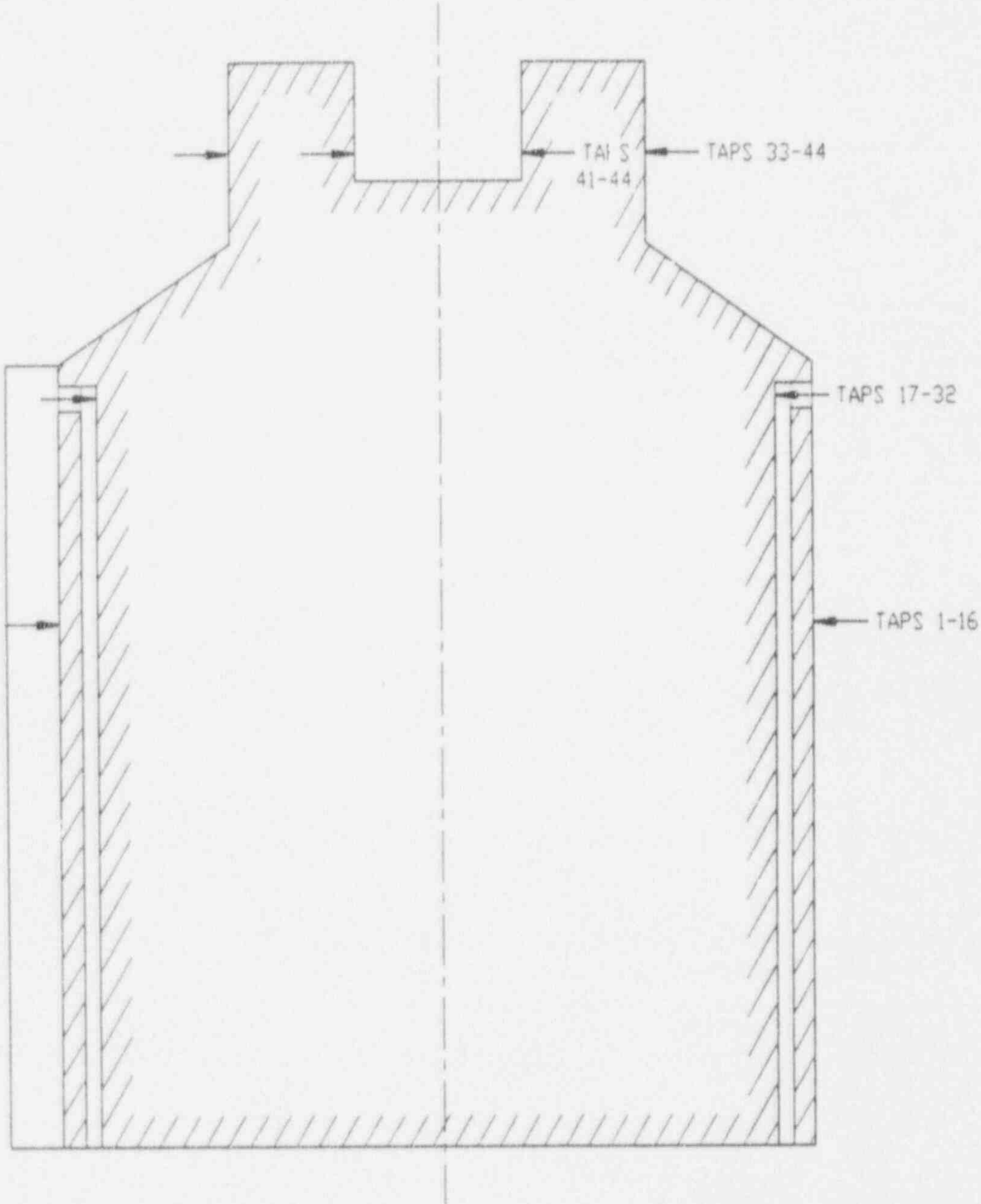

FIGURE 10a VERTICAL SECTION THROUGH THE MODEL SHOWING THE LOCATIONS OF THE PRESSURE TAP LEVELS

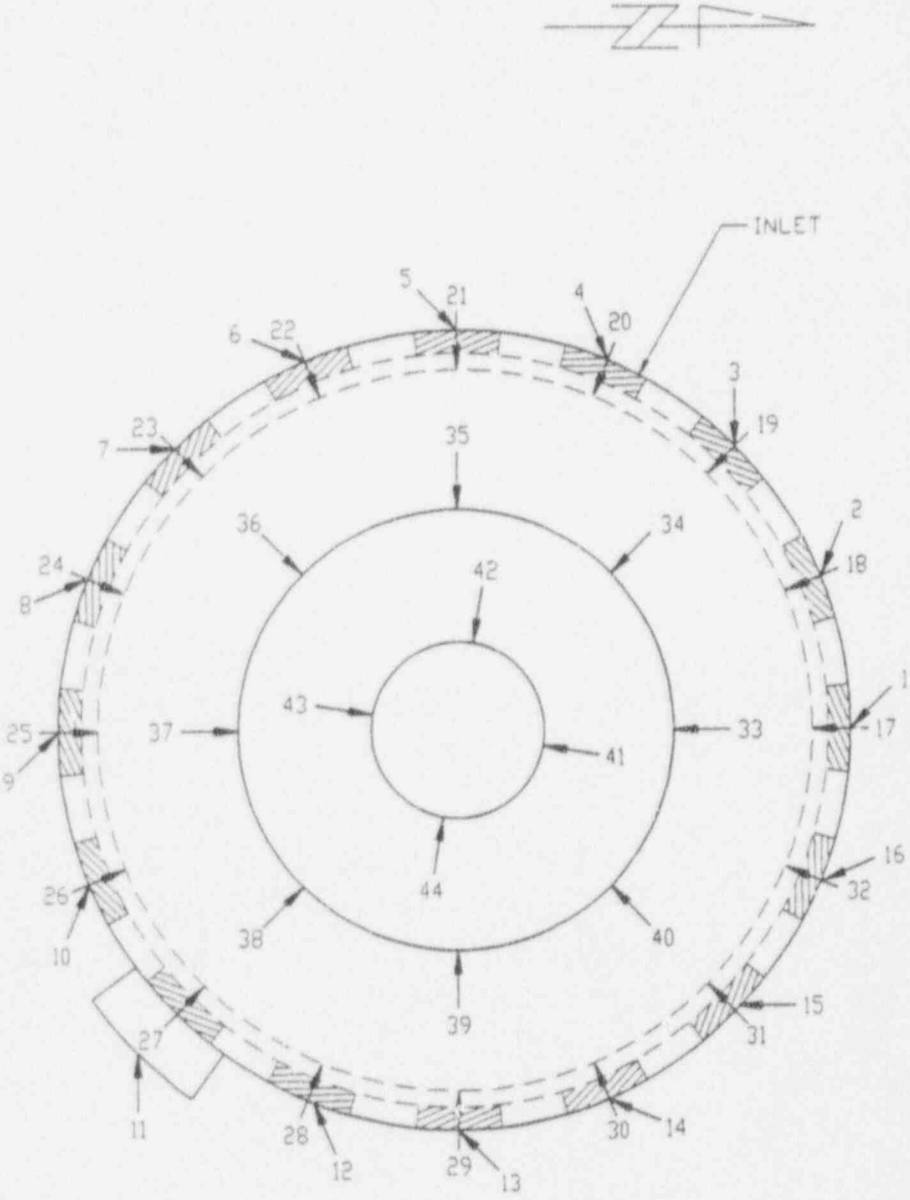

FIGURE 10b PLAN VIEW OF THE MODEL SHOWING THE PRESSURE TAP NUMBERING